

# Volumetric storage limits and space-volume multiplexing trade-offs for holographic channels

**Shayan G. Srinivasa**

**Omid Momtahan**

**Arash Karbaschi**

**Steven W. McLaughlin**

**Faramarz Fekri**

**Ali Adibi**, MEMBER SPIE

Georgia Institute of Technology

School of Electrical and Computer Engineering

777 Atlantic Drive

Atlanta, Georgia 30332

E-mail: shayan.gs@gmail.com

**Abstract.** We consider M-ary signaling in page-oriented holographic storage systems that multiplex pages using three methods: conventional angular multiplexing throughout the volume, localized recording, and a combination of angular multiplexing within localized recording. We study the mutual information transfer, which is increasingly easy to achieve in practice, between the recorded and recovered data, and use it to assess the storage density in these systems. We use the existing holographic channel model for the dominant Rician noise case for deriving the mutual information bound on the capacity and examine the interplay between the storage density and the number of recorded pages within the medium. We quantify through information-theoretical analysis that it is possible to obtain considerably higher storage capacities using gated localized holography than what can be achieved in conventional volume holography with angular multiplexing by appropriately optimizing the number of intensity levels for a given material constant and signal-to-noise ratio. © 2010 Society of Photo-Optical Instrumentation Engineers. [DOI: 10.1117/1.3294886]

Subject terms: volume holographic storage; channel capacity.

Paper 080570RR received Jul. 19, 2008; revised manuscript received Nov. 23, 2009; accepted for publication Dec. 3, 2009; published online Feb. 1, 2010.

## 1 Introduction

The advent of different data storage technologies such as volume holographic storage, solid state flash memories, and giant magnetoresistance,<sup>1</sup> holds promise for realizing enhanced data storage densities catering to future needs, and they are potential alternatives to the present day magnetic storage devices. Currently, perpendicular recording-based magnetic storage devices can support around 250 Gbits/in.<sup>2</sup> data per platter with readout speeds of 300 Mbits/s. On the other hand, solid state flash memories, such as microSD flash memories, have a capacity of 16 Gbits and can support transfer rates of ~100 Mbits/s. Inphase Technologies<sup>2</sup> has revealed practical holographic drives with 500 Gbits/in.<sup>2</sup> capacity and data transfer rates around 20 Mbits/s. Advanced research and development in data storage is still continuing for realizing high-density compact storage devices with fast data access rates. Holographic memories offer many advantages in terms of high data storage densities (1 Tbits/in.<sup>2</sup>) and high data rates<sup>3</sup> (1 Gbits/s) and could be a viable alternative for archiving data and compete with conventional data recording technologies.

In holographic storage, digital information is replicated as an optical interference pattern within a holographic material.<sup>4,5</sup> Because data are stored within the volume of the medium as opposed to that on the surface, higher storage densities can be realized. During the retrieval of data, an entire data page can be accessed at once. Thus, high data rates can be realized. There are very few practical holographic storage systems that have been demonstrated.<sup>2,3</sup>

More innovations in the fabrication of optical holographic materials and components, the development of advanced coding and signal processing algorithms, and the design of efficient system architectures needs to be done to realize a device approaching the theoretical limits.

Photorefractive crystals have been traditionally favored for rewritable holographic memories.<sup>3</sup> Among these materials, LiNbO<sub>3</sub> doped with iron has attracted a lot of attention.<sup>3</sup> Volume holograms are recorded using a reference beam (e.g., a simple plane wave) and a signal beam (containing the information). The angle of incidence of the reference beam can be varied for recording different data pages. This technique is called angular multiplexing. Retrieval of information pages can be accomplished by illuminating the medium with the same reference beam that was used for creating the hologram. The main drawback of using LiNbO<sub>3</sub>:Fe is the erasure of the holograms during the readout. Gated holography in LiNbO<sub>3</sub> was developed to address the destructive readout problem.<sup>6</sup> In this method, holograms are recorded using the reference and the signal beams in the presence of a sensitizing beam having a lower wavelength compared to the wavelength of the recording beams. This sensitizing beam acts as a gating signal that enables the recording and erasure of the holograms. Thus, during the readout with the reference beam, the holograms will not be erased. This method has been implemented with two-step recording<sup>6</sup> in pure or singly doped LiNbO<sub>3</sub>, and more recently with two-center recording<sup>7,8</sup> in doubly doped LiNbO<sub>3</sub>. The latter method, however, provides much better recording and reading performance in terms of ultimate diffraction efficiency, recording speed, and durability of the holograms.<sup>9</sup>

In conventional multiplexing methods, different holograms share the entire volume of the recording medium, making it difficult for selective recording and erasure of holograms. Recently, localized recording of holograms using two-center recording in doubly doped LiNbO<sub>3</sub> was demonstrated.<sup>10</sup> The necessity of the gating beam in two-center recording enables localized thin slices along the crystal within which individual holograms can be recorded. These slices are well separated, enabling selective recording and erasure of holograms using a gating beam for each slice of the crystal. Throughout this paper, we refer to localized recording as a new technique that allows the presence of the recording beams over a large volume of the holographic material but the actual recording is achieved only over a localized volume defined by the sensitizing (or gating) beam. Our scheme is different from other localized recording schemes that limit the volume of the material exposed to the recording beams.

Despite the unique advantage of localized recording in providing the dynamic erasure features, this scheme has not been extensively used due to loss in storage capacity<sup>10</sup> with the exception of localized recording used in a disk-based geometry in InPhase products. Initial studies<sup>10</sup> have shown that the practical limitations for reducing the thickness of the slice results in localized holograms with a large signal-to-noise ratio (SNR) (more than required), suggesting the use of gray scale coding for achieving higher storage densities. On the other hand, there have been some efforts in using multilevel (M-ary) coding for holographic storage using a conventional angular multiplexed system with not much improvement in the storage capacity due to low SNR of individual holograms.<sup>11</sup> Combining these two observations suggests that it might be possible to achieve high storage capacities by using localized recording (with large SNR per hologram) with M-ary signaling. We discuss the geometry of our localized recording in detail later in the paper.

From a communications standpoint, the entire process of sending information, storing it as a hologram, and receiving it at the detector is just another instance of a noisy communications channel. The ultimate limit for the storage and transmission of information is determined by the noise floor in the channel. We need to compute information-theoretic limits for predicting the amount of data storage and for designing multilevel codes that can achieve these limits. With the introduction of advanced coding techniques, such as low-density parity check codes,<sup>12</sup> two-dimensional multilevel constrained modulation codes,<sup>13</sup> and multilevel coding,<sup>14,15</sup> it is possible to come very close to the theoretical limits given in this paper using practical algorithms.

The achievable storage density depends on (i) the channel capacity and (ii) the physical volume of the holographic medium. The channel capacity ultimately determines the amount of information that can be stored within the medium. If the channel capacity is zero, then irrespective of system enhancements, zero storage density is realized. Thus, the capacity of holographic channels is an important property to understand the physical limits for data storage. We believe that this study will strengthen system-level design so that an appropriate choice of M-ary parameters can be made for handling system considerations such as detector and decoder complexities. In a prior work, Miridonov

et al.<sup>16</sup> considered the information capacity of holograms in photorefractive crystals based on the analog model with a continuous complex carrier. Neifeld and Chou<sup>17</sup> used the model in Ref. 18 for dominant Rician noise as well as a simple Gaussian noise model for dominant detector noise, for studying the effect of binary signaling and the efficacy of Reed Solomon codes for error correction. Burr et al.<sup>19</sup> used gray-scale recording to experimentally demonstrate performance gains over nonbinary recording by controlling the recording exposure of an individual pixel within a binary spatial light modulator (SLM). King et al.<sup>20</sup> and King and Neifeld<sup>21</sup> used nonbinary sparse permutation codes in holographic memories for demonstrating additional coding gains over the binary case.

In this paper, we use the transmission model for the digital holographic channel developed by Heanue et al.<sup>18</sup> and derive a lower bound for the channel capacity. The model developed in Ref. 18 is for the dominant optical scattering noise (Rician noise). This assumption holds true for data storage systems with thick holographic recording media producing more optical scattering noise and large diffraction power dominating the detector noise. The localized holographic data storage system has both these properties. Using this bound, we examine the trade-off between the storage density and multiplexing. We jointly optimize the number of recorded pages and the number of levels of a multilevel modulation code for maximizing the storage density. This paper is organized as follows. In Section 2, we review the transmission model for holographic channels and motivate M-ary modulation codes for holography. In Section 3, we determine the independent identically distributed (i.i.d.) capacity of holographic channels based on the channel model. In Section 4, we present a theoretical analysis for maximizing the volumetric storage density by examining the storage density versus multiplexing trade-off. We summarize the results in Section 5.

## 2 Transmission Model

In this section, we review the transmission model developed by Heanue et al.<sup>18</sup> We note a few observations for system optimization toward the end of this section and adopt this model in our subsequent analysis. The transmitted signal amplitude is represented as a vector of magnitude  $A$ . The noise is assumed to be predominantly due to optical scattering and is represented as a sum of random vectors. The magnitude  $r$  of the received signal is represented as the vector addition of the signal amplitude  $A$  and a resultant random noise phasor. The noise is characterized by a circularly symmetric Gaussian probability distribution. The detector is a square-law device that records the intensity  $y = r^2$  of the received signal. Assuming that the magnitude and phase of the received signal are statistically independent, the probability density function (pdf) of the magnitude  $r$  of the received vector is given by<sup>18</sup>

$$p_R(r) = \frac{r}{\sigma^2} \exp\left(-\frac{r^2 + A^2}{2\sigma^2}\right) I_0\left(\frac{rA}{\sigma^2}\right), \quad (1)$$

where  $I_0$  is the zero-order modified Bessel function of the first kind and  $\sigma^2$  is the noise variance. Equation (1) is a Rician pdf commonly seen in wireless communication systems.<sup>22</sup>

At the CCD, the detected signal is the light intensity whose pdf is given by

$$p_Y(y) = \frac{1}{2\sigma^2} \exp\left(-\frac{y+A^2}{2\sigma^2}\right) I_0\left(\frac{\sqrt{yA^2}}{\sigma^2}\right). \quad (2)$$

In practical systems, the medium is of finite extent. Thus, finite aperture produces optical blur, resulting in spatial intersymbol-interference (ISI). Following the work in Ref. 23, we briefly discuss the channel model for the 2-D ISI case and use this in our subsequent analysis.

### 2.1 Intersymbol-Interference Model

The spatial sampling rate is determined by the spacing of the pixels in the SLM. Let  $\Gamma$  denote the spacing of SLM pixels. Let  $g_{\text{SLM}}$  denote the linear fill factor of SLM pixel. Let  $D_N = \lambda f / \Gamma$  denote the Nyquist aperture length, where  $\lambda$  and  $f$  denote the source wavelength and the lens focal length, respectively, in a 4-F configuration.<sup>23</sup> We assume that the system has a space-invariant impulse response solely due to the aperture of area  $D^2$ . The pixel-spread function is the convolution of the space-invariant impulse response (due to the aperture) with the original pixel shape. The space-invariant impulse response is determined by the continuous space Fourier transform of the aperture shape. With a square aperture, the impulse response is an integrated 2-D separable sinc function given by

$$h(x, y) = c^2 \int_{-(1/2)g_{\text{SLM}}}^{(1/2)g_{\text{SLM}}} \int_{-(1/2)g_{\text{SLM}}}^{(1/2)g_{\text{SLM}}} \sin c \left[ \frac{D}{D_N} (x - x') \right] \times \sin c \left[ \frac{D}{D_N} (y - y') \right] dx' dy', \quad (3)$$

where,  $\text{sinc}(x) = \sin(\pi x) / \pi x$ , the variables  $x$ ,  $x'$ ,  $y$ , and  $y'$  are in the units of the pixel dimensions, and the normalizing constant  $c$  is chosen so that  $\int_{-\infty}^{\infty} \int_{-\infty}^{\infty} h^2(x, y) dx dy = 1$ .

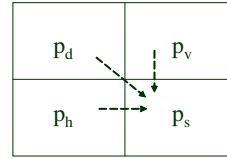
Let  $g_{\text{CCD}}$  denote the linear fill factor of the CCD detector pixel. The received signal intensity is dependent on the ISI contribution due to the horizontal, vertical, and diagonal neighbors. The amount of ISI admitted will increase as  $D \rightarrow D_N$ . We assume a one-neighbor 2-D ISI contribution to facilitate a tractable 2-D ISI analysis. This is valid as long as aperture sizes are large.

Figure 1(a) shows the first-order two-dimensional ISI configuration. The received signal at a certain pixel location is dependent on the contributions from the neighboring pixels in the horizontal, vertical, and diagonal directions. Figure 1(a) shows the basic kernel, which is a 2-D sinc function computed from Eq. (3).

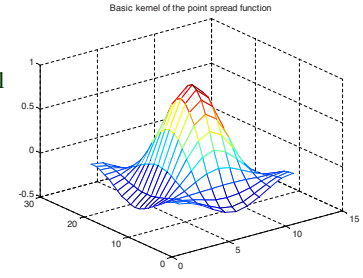
Let  $p_s$ ,  $p_h$ ,  $p_v$ , and  $p_d$  denote the self, horizontal, vertical, and diagonal pixel intensities in the configuration of Fig. 1(a). The received signal  $r_s$  due to  $p_s$  and its ISI neighbors is given by

$$r_s = \int_{-(1/2)g_{\text{CCD}}}^{(1/2)g_{\text{CCD}}} \int_{-(1/2)g_{\text{CCD}}}^{(1/2)g_{\text{CCD}}} [\sqrt{p_s} h(x, y) + \sqrt{p_h} h(x+1, y) + \sqrt{p_v} h(x, y+1) + \sqrt{p_d} h(x+1, y+1)]^2 dx dy. \quad (4)$$

Let  $x_H$  and  $x_L$  denote the intensities diffracted by the medium for the ‘‘On’’ and ‘‘Off’’ pixels, respectively, under



(a) 1<sup>st</sup> order 2-D ISI model



(b) 2-D ISI kernel

**Fig. 1** (a) Intersymbol-interference configuration and (b) ISI kernel.

ISI conditions. Define the SNR  $S = x_H / 2\sigma^2$  and the contrast ratio  $c = x_H / x_L$ . We note that this definition of the SNR is actually peak SNR and is a commonly used definition in the optics community unlike the average SNR used in communication systems. For consistency, we adhere to the peak SNR definition<sup>18</sup> in our analysis. Let  $\tilde{y} = y / x_H$  be the normalized detected intensity. Using these definitions in Eq. (2), the pdf for the normalized detected intensities of the On and the Off pixels are, respectively,<sup>18</sup>

$$p_1(\tilde{y}) = S \exp[-S(\tilde{y} + 1)] I_0(2S\sqrt{\tilde{y}}), \quad (5)$$

$$p_0(\tilde{y}) = S \exp\left[-S\left(\tilde{y} + \frac{1}{c}\right)\right] I_0\left(2S\sqrt{\frac{\tilde{y}}{c}}\right). \quad (6)$$

Figures 2(a) and 2(b) show the pdf of the On and Off pixels evaluated for different contrast ratios at a 5-dB SNR. Maintaining an infinite contrast ratio is preferred because the probability of error is minimized for signal detection due to decreased overlapping pdf regions. However, in practical systems, we always have a finite contrast ratio, making the detector design more challenging.

### 2.2 Optimal Placement of Intensities

In the M-ary encoding scheme, each SLM pixel can take one out of  $M$  intensity levels. At the detector, the received intensity should be properly distinguished and mitigate the cross talk from the neighboring pixel intensities.

One of the points of interest in M-ary coding is the spacing of the intensity levels to minimize the bit-error rate. There are two simple possibilities: equal spacing in amplitudes and equal spacing in intensities.

When the SLM amplitude levels are equally spaced, the intensity levels are quadratically spaced. The intensity level  $x_m$  for the  $m$ 'th level is given by

$$x_m = \left( \sqrt{x_L} + m \frac{\sqrt{x_H} - \sqrt{x_L}}{M-1} \right)^2. \quad (7)$$

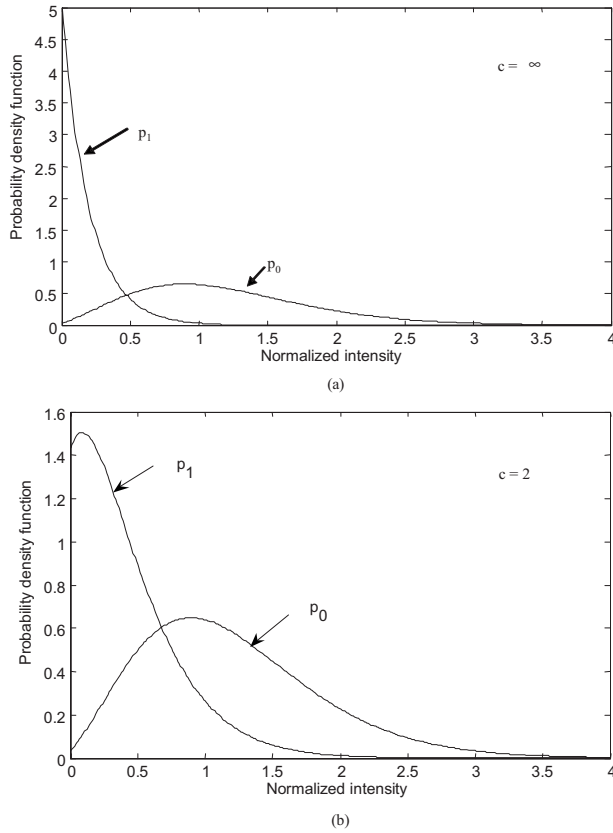


**Fig. 2** Probability density function of the received intensity at SNR = 5 dB with (a)  $c = \infty$  and (b)  $c = 2$ . The neighboring pixels are assumed to be “Off” in this example.

When the intensity levels are equally spaced, the intensity level  $x_m$  for the  $m$ 'th level is given by

$$x_m = x_L + m \frac{x_H - x_L}{M - 1}. \quad (8)$$

The variance in the detected intensity depends on the transmitted signal. From Eq. (2), the standard deviation of the detected intensity can be computed as<sup>18</sup>

$$\sigma_y^2 = 4\sigma^2(\sigma^2 + A^2). \quad (9)$$

From Eq. (9), we infer that the variance in the intensity of the detected signal depends on the intensity of the transmitted signal. Simulation results suggest a uniform spacing of the transmitted amplitude levels for a decreased probability of error.<sup>18</sup> Why is this choice practically appealing? Because amplitude levels are uniform, the intensity levels are quadratically (i.e., nonuniformly spaced). Using a threshold detector for classification, the farther the pdfs are separated, the minimal would be the overlapping regions between the pdfs and, hence, lesser would be the probability of error when doing an M-ary classification task.

In a more general setup, the intensity levels can be chosen as  $x = \{a_0 x_H, a_1 x_H, \dots, a_{M-2} x_H, x_H\}$  where  $a_0 < a_1 < \dots < a_{M-2}$  and  $a_0 = x_L / x_H$ . Each value  $a_i$  must be chosen such that the overall bit error rate is minimized according to the following:

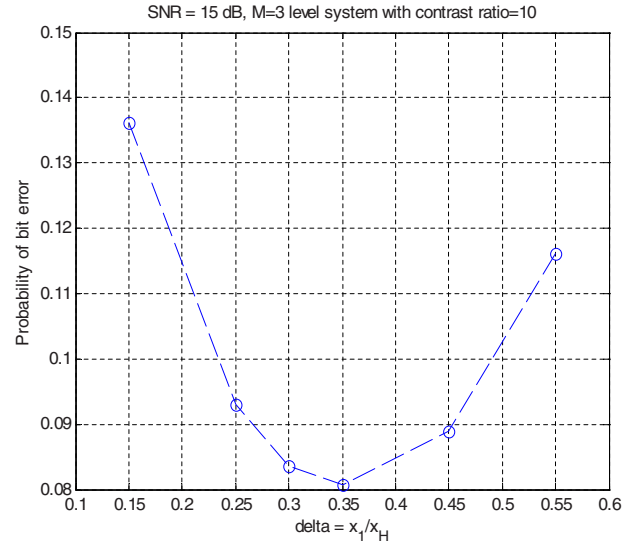


**Fig. 3** Optimal choice of intensities for a three-level system with contrast ratio of 10.

$$\bar{a} = \min_{a_0, a_1, \dots, a_{M-2}} \left[ \sum_{m=0}^{M-1} \frac{1}{M} \int_0^{\tau_m} p_m(\bar{y}) d\bar{y} + \int_{\tau_{m+1}}^{\infty} p_m(\bar{y}) d\bar{y} \right]. \quad (10)$$

where  $\tau_m$  is the the threshold between level  $m$  and  $m - 1$ .

A general analytical solution to such an optimal placement strategy for the intensities is a nonlinear multivariable optimization problem. However, for small values of  $M$ , we can optimize the placement of intensities. We consider a three level system as in Ref. 20.

Figure 3 shows the probability of error using a simple threshold detector as a function of the parameter  $\delta = a_1$ . We observed that under the operating conditions, we obtained an optimal value of  $a_1 = 0.35$  using the thresholds  $[\tau_1, \tau_2] = [0.224, 0.65]$  against a value 0.25 obtained using a uniform amplitude placement scheme. This optimization provided a slightly improved raw bit-error rate. Doing a similar optimization with  $c = \infty$  gave  $a_1 = 0.3$ .

The pdf of the normalized intensity for  $m$ 'th level after optimization is given by

$$p_m(\bar{y}) = S \exp[-S(\bar{y} + a_m)] I_0(2S\sqrt{\bar{y}a_m}). \quad (11)$$

### 3 Holographic Channel Capacity and Volumetric Storage Density

We are interested in the theoretical limits for the amount of information that can be physically stored in and retrieved from a holographic memory<sup>24</sup> with a negligible probability of error. In other words, the entire process of storing and retrieving information from a holographic memory can be viewed as transmitting a message over a 2-D channel such that the encoded source message is reconstructed from the output with a low probability of error. The channel capacity<sup>25</sup> (in bits per channel use) is the maximum rate at which this encoding and decoding can be reliably done. Specifically, in the case of data storage, this quantity gives

us a metric on the average number of bits that can be written and read reliably (i.e., with negligibly small probability of error) from the medium.

Let  $x$  be the input to the channel. The channel is characterized by the conditional probability distribution of the output  $y$  given the input  $x$  over the entire range of the input [i.e.,  $p(y|x)$ ].

To determine the holographic channel capacity, we need to determine the *a priori* probability distribution of the input  $p(x)$  that maximizes the mutual information  $I(x;y)$  between the input and output.<sup>25</sup> In other words,

$$C = \sup_{p(x)} I(x;y). \quad (12)$$

Because we need a continuous input channel description, we analyze the capacity based on the channel model presented in Ref. 18. The resulting capacity computation is a lower bound on the true holographic channel capacity because we consider uniform *a priori* distribution over a finite set of alphabets. In this section, we compute a lower bound for the channel capacity and discuss the achievability of the lower bound using practical code constructions. We also define volumetric storage density based on the channel capacity computations and SNR.

### 3.1 Capacity Lower Bound

In this section, we analyze the holographic channel capacity. Let  $\mathcal{N}_s$  denote the neighbors of the pixel  $p_s$  contributing to ISI. Enumerating the received intensity for all possible choices of  $p_s$  and  $\mathcal{N}_s$ , using Eq. (4) and plugging it into the conditional pdf of Eq. (11), we can compute a lower bound on the capacity  $C$  of holographic channels. The following result provides a lower bound on the holographic channel capacity as a function of the SNR.

**Fact 3.1.** The capacity  $C$  of a holographic channel is lower bounded by

$$C \geq \sup_M \left\{ -\frac{1}{M^{1+|\mathcal{N}_s|}} \sum_{p_s, \mathcal{N}_s} h(\tilde{y}|p_s, \mathcal{N}_s) - \int_0^\infty p(\tilde{y}) \log_2[p(\tilde{y})] d\tilde{y} \right\},$$

where  $p(\tilde{y}) = \sum_{p_s, \mathcal{N}_s} p(\tilde{y}|p_s, \mathcal{N}_s) p(p_s, \mathcal{N}_s)$  and  $h(\tilde{y}|p_s, \mathcal{N}_s) = -\int_0^\infty p(\tilde{y}|p_s, \mathcal{N}_s) \log_2[p(\tilde{y}|p_s, \mathcal{N}_s)] d\tilde{y}$ .

*Proof.* To get a computable lower bound, we pick a particular family of probability distributions and compute the mutual information. By choosing a uniform probability distribution at the input, the *a priori* probability of each SLM intensity level is  $1/M$  for all the  $M$  levels. The mutual information computed for a uniform distribution is called the i.i.d. capacity<sup>25</sup> of the channel ( $C_{i.i.d.}$ ) and will always be a lower bound on the true capacity. We use the probability distribution in Eq. (11) to compute the i.i.d. capacity as

$$C_{i.i.d.}(M) = I(x;\tilde{y}) = h(\tilde{y}) - h(\tilde{y}|x), \quad (13)$$

where  $h(\tilde{y})$  and  $h(\tilde{y}|x)$  are the differential and conditional differential entropies, respectively.

Because Eq. (11) is the conditional pdf for a certain intensity level, the overall pdf of the detected intensity is given by

$$p(\tilde{y}) = \sum_{p_s, \mathcal{N}_s} p(\tilde{y}|p_s, \mathcal{N}_s) p(p_s, \mathcal{N}_s). \quad (14)$$

Because each of  $p_s$  and its neighbors can take any  $M$ -ary value and are independent,

$$p(p_s, \mathcal{N}_s) = \frac{1}{M^{1+|\mathcal{N}_s|}}. \quad (15)$$

The conditional pdf in Eq. (14) is calculated as

$$p(\tilde{y}|p_s, \mathcal{N}_s) = S \exp \left[ -S \left( \tilde{y} + \frac{r_s}{r_s^*} \right) \right] I_0 \left( 2S \sqrt{\tilde{y} \frac{r_s}{r_s^*}} \right), \quad (16)$$

where  $r_s^*$  is the maximum value of  $r_s$  over all possible  $M$ -ary values under the ISI conditions. Using Eqs. (15) and (16) in Eq. (14), we compute the differential entropy terms in Eq. (13) as

$$h(\tilde{y}) = - \int_0^\infty p(\tilde{y}) \log_2[p(\tilde{y})] d\tilde{y} \quad (17)$$

$$h(\tilde{y}|x) = - \frac{1}{M^{1+|\mathcal{N}_s|}} \sum_{p_s, \mathcal{N}_s} \int_0^\infty p(\tilde{y}|p_s, \mathcal{N}_s) \log_2[p(\tilde{y}|p_s, \mathcal{N}_s)] d\tilde{y}. \quad (18)$$

Substituting Eqs. (17) and (18) into Eq. (13) and choosing the level  $M$  that maximizes the mutual information transfer for a given SNR, the proof holds true.  $\square$

### 3.2 Mutual Information Computation: With 2-D ISI

In this section, we will evaluate the mutual information rates for under the ISI conditions described in Fig. 1(a). Because the number of terms for the evaluation of 2-D  $M$ -ary ISI capacity increases exponentially with  $M$  and the span of 2-D ISI, we consider small values of  $M \leq 8$  with first-order 2-D ISI for our evaluation.

Figure 4 shows the i.i.d. capacity curves for  $M \leq 8$  with the parameters  $g_{SLM} = g_{CCD} = 0.9$  and  $D/D_N = 1.4$ . As we can observe from the plot, for a given number of levels  $M$ , the i.i.d. capacity converges to  $\log_2(M)$  at high SNRs. This observation can be explained as follows. When the noise floor approaches zero, the output is a close replica of the input. The mutual information reduces to computing self-entropy of the source. Assuming a uniform prior distribution, the self-entropy is  $\log_2(M)$  bits.

We note that  $C_{i.i.d.}$  is not a monotonically increasing function of the modulation level  $M$ . This fact can be observed in Fig. 4. This is because we are fixing the input distribution to be uniform. Only when the channel description is exactly known for real continuous inputs, can the prior distribution of the input be chosen to maximize the mutual information according to Eq. (12).

Fact 3.1 is useful because we can guarantee a certain upper limit for the achievable information rate over a given

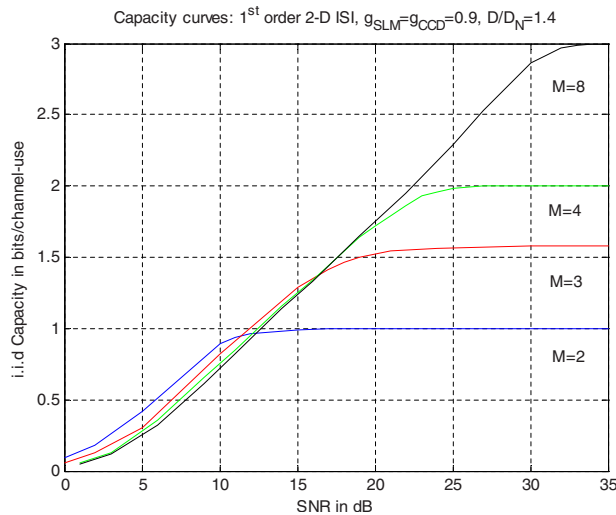


**Fig. 4** Mutual information rates for 2-D ISI case with  $g_{\text{SLM}}=g_{\text{CCD}}=0.9$  and  $D/D_N=1.4$ .

SNR using an M-ary modulation code along with an error correcting code that can give an arbitrarily small error probability. Before we conclude this section, we note that the general theoretical framework for 2-D ISI capacity computation is not yet known and is considered a hard problem in information theory. The mutual information bound is a reasonable choice for channel capacity computations for small values of  $M$  over the SNR regions of interest.

### 3.3 Volumetric Storage Density

The overall storage density  $D_s$  in a medium depends on the number of pages recorded, the number of pixels per page, and the average code rate. The achievable rate  $R(S)$  (bits per channel use) in a system is a function of the SNR ( $S$ ). The number of recorded pages  $P$  per unit volume is a function of the diffraction efficiency and is related to the SNR of the system.

Suppose each data page has  $B$  pixels per page coded at an average rate  $R$ . Then, the overall storage density  $D_s$  in bits per unit volume for a holographic memory with  $P(S)$  pages per unit volume is given by

$$D_s = P(S)BR(S). \quad (19)$$

The number of SLM pixels per page is fixed. Using Fact 3.1, we can compute  $R(S)$ . The next step is to compute  $P(S)$  and optimize  $D_s$  for a given SNR. The number of recorded pages is limited by the diffraction efficiency<sup>3</sup> and the choice of the recording mechanism. Because the diffraction efficiency is directly proportional to the readout power of the holograms, higher diffraction efficiencies imply higher SNRs. This means we can have higher volumetric storage densities with increased SNRs.

## 4 Density versus Multiplexing Trade-off Analysis

We examine volume recording with angular multiplexing<sup>3</sup> and localized recording<sup>10,26</sup> from a SNR point of view, as follows:

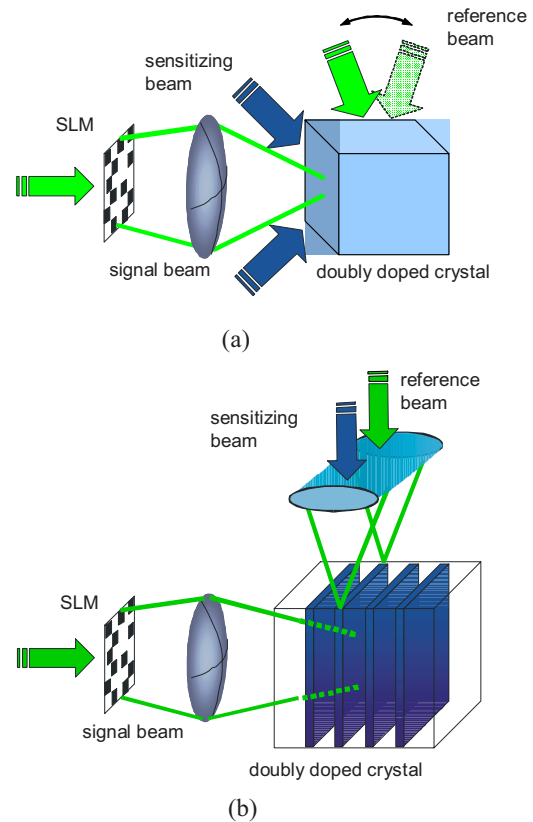


**Fig. 5** (a) Angular multiplexing volume holography using a two-center recording: holograms overlap over the entire volume of the doubly doped crystal. (b) Localized holography: holograms are recorded within the slices along the doubly doped crystal.

1. In angular multiplexed holography, several holograms share the entire volume of the holographic medium, as illustrated in Fig. 5(a). The diffraction efficiency of each hologram is inversely proportional to the square of the number of recorded holograms.<sup>27</sup>
2. In localized holography, each hologram is recorded within a thin slice of the medium, as shown in Fig. 5(b). The diffraction efficiency of a hologram in localized recording is inversely proportional to the number of recorded holograms<sup>28</sup> This is because the diffraction efficiency of the localized holograms, which are recorded in 90-deg geometry,<sup>29</sup> is proportional to the product of the thickness of the slices and the constant crystal width along the diffraction direction<sup>28</sup> The retrieved data are diffracted along the direction of the reference beam [right side of Fig. 5(b)].

Localized holography offers the unique advantage of selective recording and erasure of holograms, which is not present in angular multiplexed volume holography. From a storage standpoint, by using localized holography, we can record a few hundred holograms compared to thousands of holograms in the angular multiplexed case. However, localized holography provides improved SNR than angular multiplexing.<sup>26</sup> By designing multilevel codes for localized holography, we can achieve higher coding gains, thereby maximizing the overall storage density.

In the following section, we examine the density versus multiplexing trade-off for the two recording schemes and suggest the optimal number of pages that should be recorded. Given the SNR budget for a material, we are interested in maximizing the density  $D_s$  by an appropriate choice of the recording mechanism, the number of pages, and the number of levels ( $M$ ) of a modulation code. To make meaningful comparisons, we will fix the dynamic range parameter ( $M/\#$ ) of the recording material<sup>30</sup> to be the same for both recording mechanisms. Let this constant value be  $\kappa$ .

#### 4.1 Localized Holography

Let us first consider localized holography. Let the number of slices (or holograms) within the volume of the recording medium be  $P_1$ . Because the diffraction efficiency of each localized hologram is  $\eta_{10}=k^2/P_1$ , the resulting SNR for localized holography  $S_{10}$  is given by

$$S_{10} = \frac{\kappa^2}{2P_1\sigma^2}. \quad (20)$$

Assuming that the channel statistics do not change with the recording mechanism, the information rate can be computed by reading off the maximum value of i.i.d. capacity for  $S_{10}$  from Fig. 4. Using Eq. (20), for a fixed  $P_1$ , the overall density for localized holography  $D_s^{(l)}$  is computed as

$$D_s^{(l)} = \frac{\kappa^2}{2\sigma^2 S_{10}} BR(S_{10}). \quad (21)$$

#### 4.2 Angle Multiplexing

We now look into the angular multiplexing case. Let  $P_a$  be the number of pages that can be multiplexed within the volume of the medium. The resulting SNR for the angular multiplexing holography  $S_a$  is given by

$$S_a = \frac{\kappa^2}{2P_a^2\sigma^2}, \quad (22)$$

because the diffraction efficiency of each hologram is given by  $\kappa^2/P_a^2$ . Using Eq. (22), the storage density  $D_s^{(a)}$  for angular multiplexing is given by

$$D_s^{(a)} = P_a BR(S_a). \quad (23)$$

Using Eq. (22) in Eq. (23), we get

$$D_s^{(a)} = BR(S_a) \frac{\kappa}{\sqrt{2\sigma^2 S_a}}. \quad (24)$$

To achieve the best storage density, we need to optimize Eq. (24) with respect to the number of pages and the number of levels. The optimum density ( $D^*$ ) is given by

$$D^* = \max_{P_a M} D_s^{(a)}. \quad (25)$$

We note that the SNR is not a free parameter. There is an optimal SNR that maximizes Eq. (25) given fixed values for  $\kappa$  and  $\sigma$ .

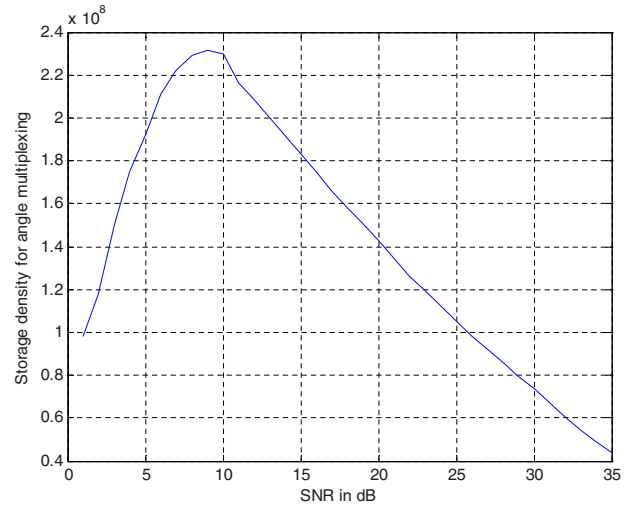


Fig. 6 Achievable storage density with angle multiplexing as a function of the SNR for  $M=2$  levels.

**Example.** We will explain this trade-off with an example. We let  $\kappa=1.1$ ,<sup>23</sup>  $c=\infty$ , and  $\sigma^2=10^{-6}$ . With the above parameters, the optimal SNR for localized recording is 4 dB. We can achieve a theoretical storage density  $D_s^{(l)}=0.085$  Tbits/volume with  $P_1=24085$  thin slices and binary recording. However, it is practically impossible to go with such thin slices due to optical limitations. Because this is a constrained optimization setup, a reasonable practical choice for the number of localized slices is around  $P_1=400$ .<sup>26</sup> The corresponding SNR is computed as  $S_{10}=40$  dB. With a projected maximum value i.i.d. capacity at 40 dB as 4.75 bits/channel use,  $D_s^{(l)}=0.2675$  Gbits/unit volume can be achieved with  $P_1=400$  using localized recording with M-ary recording.

Following the optimization in Eq. (25) for angular multiplexing, for the parameters in this example, the SNR that maximizes storage density is 9 dB. We estimate that a storage density of 0.231 Gbits/unit volume can be realized using binary recording over 276 pages. Under similar ISI conditions, the experimental density is estimated at 400 bits/ $\mu\text{m}^2$ ,<sup>23</sup> which is relatively close. With 627 pages of 3-ary encoding our density estimates are 0.13 Gbits/unit volume as against 0.84 Gbits reported in Ref. 20. These variations in estimates could be due to factors in modeling a real system most accurately. Figure 6 shows the optimization results for the overall storage density for the binary case. The number of recorded pages is thus directly related to the SNR of the medium. With  $\kappa=3$ ,<sup>9</sup> we can however record 752 pages achieving a maximum storage density of 0.63 Gbits/vol using binary recording.

Thus, given two different recording schemes with the same material and constraints, localized recording seemed better in this example. The above theoretical analysis can be worked out for different practical choices of the system parameters and SNRs. The examples are suggestive to show the constrained optimization trade-offs.

#### 4.3 Angular Multiplexing within Localized Recording

We also look into the case where we have combined localized recording and angular multiplexing. In this hypoth-

esized recording scheme, the crystal is divided into a number of thin slices and holograms are angularly multiplexed within each slice. We investigate the SNR and storage density that can be achieved in this scheme.

Let the number of thin recording slices be  $P_1$ . Let  $P_a$  be the number of holograms that can be multiplexed within each slice. Let  $D_s^{(la)}$  be the optimized achievable storage density for angular multiplexing within localized recording. The SNR for this scheme is given by

$$S_{la} = \frac{\kappa^2}{2P_a^2 P_1 \sigma^2}. \quad (26)$$

Fixing  $P_1$  and optimizing the storage density  $D_s^{(la)}$  over all choices of  $P_a$  and the choice of multilevel code, we have

$$D_s^{(la)} = \max_{P_a M} P_a P_1 B R(S_{la}). \quad (27)$$

**Example.** In this example, we will compute the optimized achievable density for this scheme. We use the same parameters as in the previous example (i.e.,  $\kappa=1.1$ ,  $c=\infty$ ,  $\sigma^2=10^{-6}$ ,  $P_1=400$ , and  $B=1$ Mbit pixels/page). Optimizing the values of  $P_a$  and  $M$ , we can theoretically achieve at least 4.63 Gbits/vol of information storage by doing a binary recording with 14 multiplexed pages per slice. This is a significant amount of data storage compared to the other two schemes. However, we need practical schemes to get to the limits predicted in this example.

## 5 Conclusions

We investigated the i.i.d. 2-D ISI capacity of holographic channels based on the Rician noise channel model. Using the existing framework of error-correction codes, we can design a combined modulation/error-correcting code for achieving the derived information-theoretic rates. We presented an analysis of the storage density versus multiplexing trade-off for three different recording schemes. Given the SNR budget for a material, this trade-off is useful for deciding the recording mechanism and then optimizing the number of pages and desired level of an M-ary code for maximizing the volumetric storage density. Our analysis shows that by appropriate optimization of the localized holographic storage system along with the proper choice of the number of intensity levels ( $M$ ) for the M-ary coding, it is possible to obtain storage capacities considerably higher than what can be achieved in conventional volume holography with angular multiplexing. Knowing the additional advantage of localized recording in providing dynamic erasure, the results of this paper suggest a new approach for optimizing the storage capacity of holographic memories. It would be a future study to build a practical coding scheme that achieves the theoretical bounds in the paper.

## Acknowledgments

This work was supported by the Air Force Office of Scientific Research under Grant No. FA9550-05-1-0438 (G. Pomrenke).

## References

1. J. Akerman, "Toward a universal memory," *Science* **308**, 508–510 (Apr. 2005).
2. K. Anderson, E. Fotheringham, A. Hill, B. Sissom, and K. Curtis, "High speed holographic data storage at 500 Gb/in<sup>2</sup>," InPhase Technologies, white paper, (<http://www.inphase-technologies.com/downloads/pdf/technology/HighSpeedHDS500Gbin2.pdf>).
3. J. Ashley, M.-P. Bernal, G. W. Burr, H. Coufal, H. Guenther, J. A. Hoffnagle, C. M. Jefferson, B. Marcus, R. M. Macfarlane, R. M. Shelby, and G. T. Sincerbox, "Holographic data storage," *IBM J. Res. Dev.* **44**, 341–368 (May 2000).
4. L. Hesselink and S. Orlov, "Photorefractive materials for nonvolatile volume holographic storage," *Science* **282**(5391), 1089–1094 (Nov. 1998).
5. D. Psaltis and F. Mok, "Holographic Memories," *Science* **273**(5), 70–76 (Nov. 1995).
6. D. vonderLinde, A. M. Glass, and K. F. Rodgers, "Multiphoton photorefractive process for optical storage in LiNbO<sub>3</sub>," *Appl. Phys. Lett.* **25**, 155–157 (1974).
7. K. Buse, A. Adibi, and D. Psaltis, "Non-volatile holographic recording in doubly doped lithium niobate crystals," *Nature (London)* **393**, 665–668 (Jun. 1998).
8. A. Adibi, K. Buse, and D. Psaltis, "Two-center holographic recording," *J. Opt. Soc. Am. B* **18**(5), 584–601 (Jun. 2001).
9. O. Momtahan, A. Karbaschi, and A. Adibi, "Gated holography: materials, techniques, and applications," *Proc. SPIE* **4988**, 24–39 (2003).
10. C. Moser, B. Schupp, and D. Psaltis, "Localized holographic recording in doubly doped lithium niobate," *Opt. Lett.* **25**, 162–164 (Feb. 2000).
11. G. W. Burr, M. A. Neifeld, G. Barking, H. Coufal, J. A. Hoffnagle, and C. M. Jefferson, "Gray-scale data pages for digital holographic data storage," *Opt. Lett.* **23**(15), 1218–1220 (1998).
12. R. G. Gallager, "Low density parity check codes," PhD Thesis, M.I.T Press, Cambridge, MA (1963).
13. S. G. Srinivasa and S. W. McLaughlin, "Capacity bounds for two-dimensional asymmetric M-ary (0, k) and (d, ∞) runlength-limited channels," *IEEE Trans. Commun.* **57**, 1584–1587 (June 2009).
14. U. Wachsmann, R. F. H. Fisher, and J. B. Huber, "Multilevel codes: theoretical concepts and system design rules," *IEEE Trans. Inf. Theory* **45**, 1361–1391 (Jul. 1999).
15. U. Wachsmann, J. B. Huber, and P. Schramm, "Comparison of coded modulation schemes for the AWGN and the Rayleigh fading channel," in *Proc. IEEE. ISIT*, Cambridge, pp. 5 (Aug. 1998).
16. S. V. Miridonov, A. V. Khomenko, D. Tentori, and A. A. Kamshilin, "Information capacity of holograms in photorefractive crystals," *Opt. Lett.* **19**, 502–504 (Apr. 1994).
17. M. A. Neifeld and W. Chou, "Information theoretic limits to the capacity of volume holographic optical memory," *Appl. Phys. Lett.* **36**, 514–517 (Jan. 1997).
18. J. F. Heanue, M. C. Bashaw, and L. Hesselink, "Channel codes for digital holographic storage," *J. Opt. Soc. Am.* **12**, 2432–2439 (Nov. 1995).
19. G. W. Burr, G. Barking, H. Coufal, J. A. Hoffnagle, C. M. Jefferson, and M. A. Neifeld, "Gray-scale data pages for digital holographic data storage," *Opt. Lett.* **23**, 1218–1220 (1998).
20. B. M. King, G. W. Burr, and M. A. Neifeld, "Experimental demonstration of gray-scale sparse modulation codes in volume holographic storage," *Appl. Opt.* **42**, 2546–2559 (2003).
21. B. M. King and M. A. Neifeld, "Low-complexity maximum-likelihood decoding of shortened enumerative permutation codes for holographic storage," *IEEE J. Select. Commun.* **19**, 783–790 (2001).
22. J. G. Proakis, *Digital Communications*, McGraw Hill, New York (2001).
23. L. Menetrier and G. W. Burr, "Density implications of shift compensation postprocessing in holographic storage systems," *Appl. Opt.* **37**, 845–860 (2003).
24. S. G. Srinivasa, O. Momtahan, A. Karbaschi, S. W. McLaughlin, A. Adibi, and F. Fekri, "M-ary, binary and space volume multiplexing tradeoffs for holographic channels," in *Proc. IEEE. Globecom.*, San Francisco, (Nov. 2006).
25. T. Cover and J. Thomas, "Elements of Information Theory," Wiley, Hoboken, NJ (1991).
26. A. Karbaschi, O. Momtahan, A. Adibi, and B. Javidi, "Optical correlation using gated localized holography," *Opt. Eng.* **44**, 1–8 (Aug. 2005).
27. D. Psaltis, D. Brady, and K. Wagner, "Adaptive optical networks using photorefractive crystals," *Appl. Opt.* **27**, 1752–1759 (May 1998).
28. C. Moser, I. Maravic, B. Schupp, A. Adibi, and D. Psaltis, "Diffraction efficiency of localized holograms in doubly doped LiNbO<sub>3</sub> crystals," *Opt. Lett.* **25**, 1243–1245 (Sep. 2000).
29. G. W. Burr, F. H. Mok, and D. Psaltis, "Angle and space multiplexed

holographic storage using 90° geometry,” *Opt. Commun.* **117**, 49–55 (May 1995).

30. F. Mok, G. W. Burr, and D. Psaltis, “System metric for holographic memory systems,” *Opt. Lett.* **21**, 896–898 (1996).



**Shayan G. Srinivasa** obtained his PhD in electrical engineering from Georgia Institute of Technology in August 2006, MS in electrical engineering from the University of Florida in 2001, and BE in electronics and communication engineering from the University of Mysore, India, in 1997 with the distinguished university rank award. He is also a National Talent Search Scholar awarded by the Government of India. He has held full-time senior engineering positions at Infosys Technologies and Broadcom Corporation. He is currently a research staff member in the read channels R&D Division at STMicroelectronics. His research interests are in the broad areas of information theory and signal processing and its applications to communication channels.

positions at Infosys Technologies and Broadcom Corporation. He is currently a research staff member in the read channels R&D Division at STMicroelectronics. His research interests are in the broad areas of information theory and signal processing and its applications to communication channels.



**Omid Momtahan** obtained his BS in electrical engineering from Shiraz University in 1996, ranking first among his graduating class. He was with the Electrical Engineering Department of Sharif University of Technology from 1996, obtaining his MS in 1998. After two years of teaching and working in industry, in 2001 he attended the School of Electrical and Computer Engineering, Georgia Institute of Technology and received his PhD in 2006 under the supervision of Prof.

Ali Adibi. Currently, he is an R&D research engineer at Avago Technologies. He is the recipient of the Outstanding Young Researcher Award from Optics in the South-east Conference, Atlanta, and Electrical and Computer Engineering Graduate Research Assistant Excellence Award from the School of Electrical and Computer Engineering, Georgia Institute of Technology, both in 2005. He also received the best paper award at the 50th IEEE Vehicular Technology Conference held in Amsterdam, in 1999. His technical interests are optical spectroscopy, biosensors, volume holographic memories, and wireless communications.



**Arash Karbaschi** received his electrical engineering PhD from Georgia Institute of Technology in 2008 and his MSc and BSc from Sharif University of Technology, Iran, in 1998 and 1996, respectively. He has performed extensive theoretical and experimental research in holography. He has been involved in optical information processing, data storage, and spectroscopy using volume holography. He was a member of the National Physics Olympiad team of Iran in 1992.



**Steven W. McLaughlin** received his BSEE from Northwestern University, MSE from Princeton University, and PhD from the University of Michigan. He joined the School of Electrical and Computer Engineering at Georgia Tech in 1996, where is now vice provost for international initiatives and Ken Byers Professor of ECE. As vice provost, he is responsible for Georgia Tech’s global engagement and is the point person for international initiatives in research, education, and economic development. His research interests are in the gen-

eral area of communications and information theory. He has had authored more than 200 journal and conference papers and holds 26 U.S. Patents. He has served as the research and thesis advisor to more than 50 students at the bachelors, masters, doctoral, and postdoctoral levels. He is a Fellow of the IEEE and served as an associate editor for coding techniques for the *IEEE Transaction on Information Theory*. He also served as the publications editor for that journal from 1995 to 1999. He coedited (with Sergio Verdu) *Information Theory: 50 Years of Discovery* (Wiley/IEEE Press, 1999). He has also served on the IEEE Publications Activities Board (1998–2001) and is a former secretary of the IEEE Atlanta Section (2000).

eral area of communications and information theory. He has had authored more than 200 journal and conference papers and holds 26 U.S. Patents. He has served as the research and thesis advisor to more than 50 students at the bachelors, masters, doctoral, and postdoctoral levels. He is a Fellow of the IEEE and served as an associate editor for coding techniques for the *IEEE Transaction on Information Theory*. He also served as the publications editor for that journal from 1995 to 1999. He coedited (with Sergio Verdu) *Information Theory: 50 Years of Discovery* (Wiley/IEEE Press, 1999). He has also served on the IEEE Publications Activities Board (1998–2001) and is a former secretary of the IEEE Atlanta Section (2000).



**Faramarz Fekri** received his BSc and MSc from Sharif University of Technology, Tehran, Iran, in 1990 and 1993, respectively, and PhD from the Georgia Institute of Technology in 2000. Since 2000, Dr. Fekri has been on the faculty of the School of Electrical and Computer Engineering at the Georgia Institute of Technology. He is a member of the Georgia Tech Broadband Institute, the Center for Signal and Image Processing, and the Georgia Tech Information Security Center. Dr. Fekri’s current research interests are in the area of communications and signal processing, in particular, error-control coding, information processing for wireless and sensor networks, and communication security. He serves on the editorial board of the *IEEE Transactions on Communications* and on the Technical Program Committees of several IEEE conferences. He has received several prestigious awards, including the Outstanding Junior Faculty Member Award of the School of ECE (2006), Southeastern Center for Electrical Engineering Education Young Faculty Development Award (2003), National Science Foundation CAREER Award (2001), and Best PhD Thesis Award of the Georgia Institute of Technology chapter of Sigma Xi (2000). He is a Senior Member of the IEEE.

Dr. Fekri’s current research interests are in the area of communications and signal processing, in particular, error-control coding, information processing for wireless and sensor networks, and communication security. He serves on the editorial board of the *IEEE Transactions on Communications* and on the Technical Program Committees of several IEEE conferences. He has received several prestigious awards, including the Outstanding Junior Faculty Member Award of the School of ECE (2006), Southeastern Center for Electrical Engineering Education Young Faculty Development Award (2003), National Science Foundation CAREER Award (2001), and Best PhD Thesis Award of the Georgia Institute of Technology chapter of Sigma Xi (2000). He is a Senior Member of the IEEE.



**Ali Adibi** is a professor in the School of Electrical and Computer Engineering and the director for the Center for Advanced Processing Tools for Electromagnetic/Acoustics Xtals at the Georgia Institute of Technology. He received his BSEE from Shiraz University (Iran) in 1990 and his MSEE and PhD from the Georgia Institute of Technology (1994) and the California Institute of Technology (1999), respectively. His PhD research resulted in a breakthrough in persistent holographic storage in photorefractive crystals. He was an assistant professor from 2002 to 2004 in the School of Electrical and Computer Engineering at the Georgia Institute of Technology, where he is now an associate professor. His research interests include holographic data storage; holographic optical elements for optical communications; 3-D optical pattern recognition; design, characterization, and applications of photonic crystals for chip-scale WDM and biosensors; spectrometers for biosensing and environmental sensing; high-resolution optical imaging for biomedical applications; ultradense and ultrafast optical interconnects; and optical communication and networking. He is a senior member of IEEE and a member of Sigma Xi, OSA, SPIE, and ASM.

His PhD research resulted in a breakthrough in persistent holographic storage in photorefractive crystals. He was an assistant professor from 2002 to 2004 in the School of Electrical and Computer Engineering at the Georgia Institute of Technology, where he is now an associate professor. His research interests include holographic data storage; holographic optical elements for optical communications; 3-D optical pattern recognition; design, characterization, and applications of photonic crystals for chip-scale WDM and biosensors; spectrometers for biosensing and environmental sensing; high-resolution optical imaging for biomedical applications; ultradense and ultrafast optical interconnects; and optical communication and networking. He is a senior member of IEEE and a member of Sigma Xi, OSA, SPIE, and ASM.